Spatial Structure of Inertial-period Motions in a Two-layered Sea, Based on Observations[1]

Friedrich Schott

Institut für Meereskunde an der Universität Kiel
2300 Kiel, Germany

ABSTRACT

Spatial coherence and phase relationships of inertial-period motions have been inferred from an experiment with four moorings in the northern North Sea where the density profile was almost two-layered. The inertial-period currents showed antiphase between the upper and lower layers; the coherence between both layers was high. The inertial-period temperature fluctuations were in phase throughout the thermocline.

These vertical relationships can be interpreted as follows: by wind action at the sea surface, internal waves are generated with frequencies that are higher than the inertial frequency, and in the course of time these frequencies approach the inertial frequency. During this frequency variation, the vertical components of the internal waves decline more quickly than do the horizontal currents. Therefore, the current oscillations contain more energy at the very small wave-numbers than do the temperature fluctuations. This is demonstrated by the horizontal phase differences of currents and temperature fluctuations.

After the free inertial oscillations were eliminated from the current records, the time series of the remaining forced near-inertial-current oscillations were compared with the variations in local winds. For one sudden wind-stress change, high forced oscillations were apparent in these time series, but after only a few cycles the energy of the forced oscillations had shifted toward the zero wave-numbers.

The horizontal wavelengths and propagational directions of the forced oscillations were determined under two different weather conditions. The wavelengths were about 50 km under both conditions observed, but the direction of propagation could not be correlated with the motions of the wind fields.

1. *Introduction.* In recent years, numerous current observations revealing inertial-period oscillations have been reported. A first review of the published data (until 1967) on their occurrence in oceans, enclosed seas, and lakes has been presented by Webster (1968). Since that time new continuous and extended records of inertial currents have been obtained under various oceanic conditions (Pollard and Millard 1970, Perkins 1970, Tomczak 1970). Nevertheless, our present knowledge is not adequate to describe satisfactorily the generation, propagation, and decay of these oscillations. The widespread observa-

1. Accepted for publication and submitted to press 1 December 1970.

tions have only shown that planetary effects and tidal generation seem to be of minor importance.

It seems to be well established now that atmospheric action at the sea surface is a primary force in generating inertial oscillations. However, an explanation of actual measurements of inertial-period currents by means of wind-stress changes has been possible for the wind-mixed near-surface layer only (Pollard and Millard 1970). But how is the energy transferred from the surface down to the deeper layers? Principle features of the vertical current profile—the usually observed small vertical coherence scale, with sometimes high inertial motions at one depth but not at another—have been well explained by K. Hasselmann's (1970) theory of the phase mixing of modes with closely neighboring frequencies. Although the experiments with vertically distributed current meters in single moorings have provided a good picture of the vertical coherence scale of inertial oscillations, our knowledge on their horizontal coherence scale is very meagre. Only two experiments that employed horizontally spaced sensors have been reported (Perkins 1970), and these were undertaken by Webster and Fofonoff of the Woods Hole Oceanographic Institution. In one case the current meters were at depths of 88 m and 98 m and the horizontal distance between the meters was 3 km; in the second case, two current meters were at a depth of 620 m and were 65 km apart. In the first case, the coherence for the inertial-period currents was 0.7, and part of the coherence loss in this case is certainly due to the 10-m depth difference between the sensors; in the second case there was no coherence. Because of this insufficient knowledge on the horizontal coherence scale of inertial motions, it is necessary to start work on the horizontal extent and coherence of inertial-period motions using closely spaced moorings. A second problem that has not yet been tackled is to derive from measurements the relationship between vertical and horizontal components of inertial-period motions.

In the present study, vertical and horizontal coherence and phase relationships of the vertical and horizontal inertial-period motions are presented, and an interpretation of the relationships between horizontal and vertical motions is attempted. In order to clarify what is meant by "inertial" in this paper, let me state that "inertial" in connection with observational analysis always means "near-inertial," since the estimates of amplitudes, coherences, and phase values always apply to a frequency band.

2. *Observations.* The data from which these relationships have been derived consist of current and temperature measurements in the northern North Sea. Three moorings (Sts. Ost, West, Süd) were arranged in a triangle around a fourth mooring (St. Mitte) in the center of the triangle at 56°20'N, 1°E; the sides of the triangle measured about 4.5 km. The water depth at the mooring positions was 82 m. The moorings were put into the water 14 September 1968 and were recovered 27 September 1968.

Table I. Equipment used in the study.

Station	Instrument number	Instrument type	Property measured*	Sensor depth (m)	Record length (hours)
West.....	2	Bergen	s, d, t	31.9	306
Ost.....	1	Bergen	s, d, t	18.3	309
	2	Bergen	s, d, t	32.4	309
Mitte.....	1	Geodyne	s, d	18.5	312
	3	Geodyne	s, d	36.0	207
	5	Geodyne	s, d	70.0	128
	6/6	Bergen	t	28.1	312
	.	(thermistor	.	.	.
	.	chain)	.	.	.
	.		.	.	.
	6/11		t	37.6†	312
Süd	2	Bergen	s, d, t	33.8	311

* s, current speed; d, current direction; t, temperature.
† Sensor distance, 1.9 m.

Table I gives the identification numbers of the instruments referred to in this study, the instrument types, the properties measured by each instrument, the sensor depths, and the record lengths in hours. The sampling interval was five minutes for all instruments.

In the following account are presented the coherence and phase differences not only between measurements recorded by instruments of the same type but also by Geodyne-type and Bergen-type meters. This difference in type should not affect the results, since a report by a SCOR Working Group (1969) has shown that only for periods of less than one hour may systematic differences between these two current-meter types be apparent due to the different sampling techniques of both instruments. The clock inaccuracies during the recording period were not more than 5 minutes for all instruments, except for meter No. 2 at St. Ost, where the deviation was 15 min; the temperature record of this instrument, which is used for the calculation of propagational direction and therefore needs an exact time base, was therefore corrected by interpolation with the correct time interval.

The salinity at the mooring positions was constant throughout the water column, and the temperature profile was almost two-layered; but the thermocline between 30 m and 37 m was of varying depth and shape. Three profiles, determined from the thermistor chain measurements at St. Mitte, are presented in Fig. 1. Each consists of mean values, taken over two tidal periods. From the density profile, the recording period can be devided into three sections: during the first section, from 14 September to 18 September, the temperature profile was similar to profile 1 in Fig. 1; from 18 September to 22 September, it was similar to profile 2; and from 22 September to 27 September the temperature had a profile like profile 3.

Wind recordings were not obtained at the mooring positions; the mean wind conditions, therefore, had to be taken from merchant-ship observations in that area (Deutscher Wetterdienst 1968b) and from weather maps (Deutscher Wetterdienst 1968a). Because of the variations in the density profile and in the wind conditions, coherence and phase values computed from the entire record are affected by a mixture of different inertial-motion events and propagational conditions. Therefore, in addition to these values of coherence and phase from the total record (14 September to 27 September), values are also given for 14 September to 18 September. During these first four days of recording, a constant density profile prevailed, and, as will be shown, the records for this time were dominated by a single inertial-motion event. Besides, for investigation of the vertical current structure, only the first days of the records can be used, because the meters below the thermocline failed to function after some days (Table I).

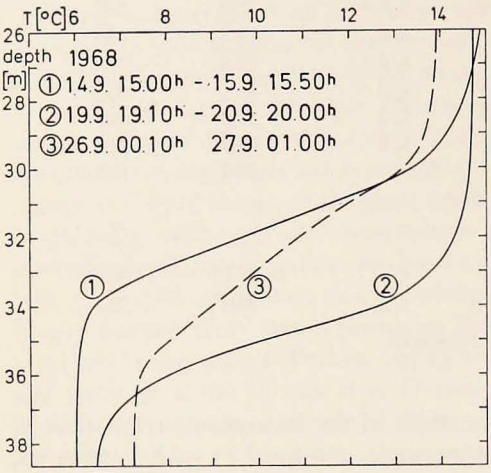

Figure 1. Three temperature profiles from the thermistor-chain records at St. Mitte. The averaging periods for the profiles are indicated in the Figure; each of the three periods equals two tidal periods.

3. *Data Analysis.* Current spectra obtained in the North Sea show a dominant peak at the semidiurnal (M_2) tidal period of 12.42 h. The local inertial period of 14.4 h at the mooring positions falls rather close to the tidal period; the tidal-current amplitudes derived from the 14 days of record are approximately four times the amplitudes of the inertial-period currents, as can be seen (Fig. 2) in the current amplitude spectrum for current meter No. 1 at St. Ost (18.3 m). Coherence and phase differences for the inertial period, computed from the short records, would therefore be considerably biased without suppression of the M_2 constituent. The normal tide-eliminating filters, such as those proposed by Doodson and Warburg (1941), are low-pass filters that also reduce the amplitudes to a small fraction at the inertial period. For this reason I have used, in the present study, the following two-step filtering procedure; it is rather rough, but it serves its purpose, as is obvious from the prefiltered records.

First, equally weighted running means, with an averaging period of 12 h 25 min, were computed from the original measurements. The frequency response, $A(\nu)$, of this procedure is

$$A(\nu) = \frac{1}{149} \frac{\sin(12 \cdot 42\pi\nu)}{\sin(\pi\nu/12)},$$

with the frequency, ν, given in cycles per hour (cph). The M_2 constituent and the higher harmonics were eliminated by this procedure. For low frequencies, the response is $A = 1$; for high frequencies, A approaches zero under alternation; and for $\nu = 12$ cph, $A = 1$ also.

Second, the hourly mean values of these prefiltered 5-min.-interval data were treated by another filter in order to take out the remaining long-period and short-period fluctuations. This was a rectangular filter, having a pass band ranging from 10 h to 18 h; the number of filter factors was 20.

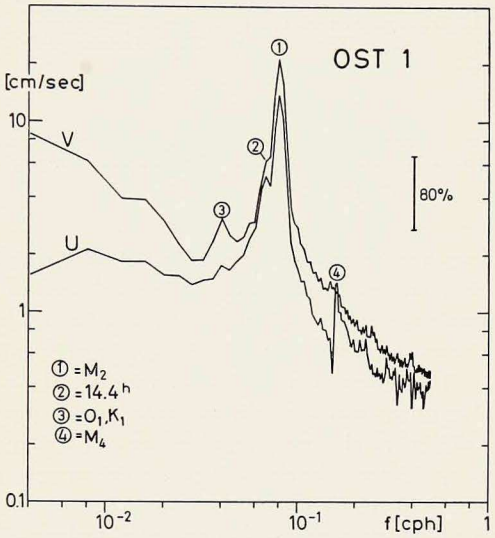

Figure 2. Current-amplitude spectra of eastward (u) and northward (v) current components at St. Ost (sensor at 18.3 m).

The frequency response of the two-step filtering process is shown in Fig. 3. The procedure of running means reduced the inertial-period amplitudes (at $\nu = 0.0695$ cph) to 17% of the original values, but, since the tides were eliminated and since other long-period and short-period fluctuations were largely removed by the two filters, only the inertial period was still of importance in the records, after the filtering. Normally, there are 20 hourly values lost at the beginning and the end of the records following application of a filter with 20 filter factors. However, just after the measurements were begun, a long calm-weather period terminated with strong winds—an interesting situation for inertial-wave studies. But how to apply the filter and not loose the information of the first 20 values?

Fig. 4 shows a cosine function (solid line) of 14.4-h period; if this curve is continued to the left with 20 values of zero amplitude and if the above-described rectangular filter is then applied, the dashed curve in Fig. 4 is the result. At first this curve differs from the cosine function, but after only a few hours the difference between the original curve and the filtered curve is very small. So, the 20 values, gained by continuation of the records at both ends, can provide useful information on the approximate size of the inertial-period variations in those parts of the original records that would otherwise be lost; such

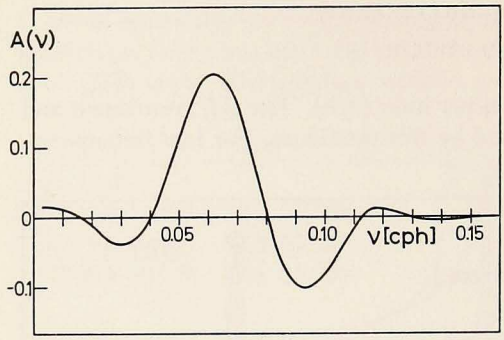

Figure 3. Frequency response of the two-step filtering process.

continuation values are shown in Figs. 5 to 8.

Fig. 5 shows the current oscillations, after filtering, for St. Ost at depths of 18.3 m and 32.4 m. They are of pure rotary type. Fig. 6 presents the temperature fluctuations, after filtering, for St. Mitte from depths of 28.1 m to 37.6 m in 1.9-m depth intervals, as obtained by the two-step filtering procedure. The filtered temperature fluctuations at about 32 m at the four moorings are given in Fig. 7. A count of the cycles shows that the periods of these fluctuations correspond to the local inertial period; for example, from 18 September, 0 h, to 21 September, 0 h, the St. Mitte record 6/9 at 33.8 m (Fig. 6) shows 5 cycles, corresponding to a period of 14.4 h.

The question might arise whether these temperature fluctuations could be due to the tilting of the moorings under the influence of inertial-period current friction at the moorings. However, the temperatures and the currents show very different horizontal phase differences between the stations, so this effect needs no further consideration.

The coherence and phase relationships, obtained from the filtered records of currents and temperatures, are presented in Tables II to V. The confidence limits for the coherences for the short records are high. When treating the whole record (14 September, 21 h, to 27 September, 3 h), the ratio of the number of lags used (m) to the number of hourly data points (n) was $m/n = 0.2$. The 95%-confidence limit for the coherence was $k = 0.73$ (see Granger and Hatanaka 1964). When treating the first part of the records (14 September, 21 h, to 18 September, 19 h), the ratio m/n was 0.33, which corresponds to a 95%-confidence limit of

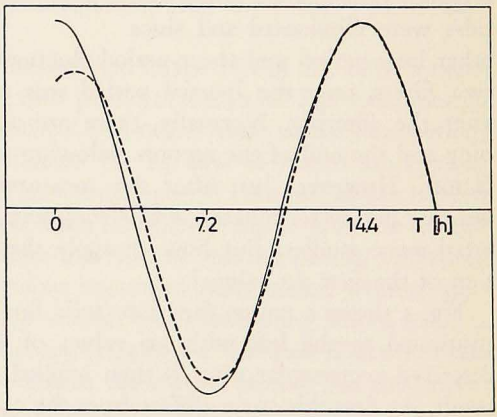

Figure 4. The results (dashed line) derived when a sine wave of 14.4-h period (solid line) is continued to the left by 20 values of zero amplitude and a filter (pass band 10–18 h, 20 filter factors) is applied.

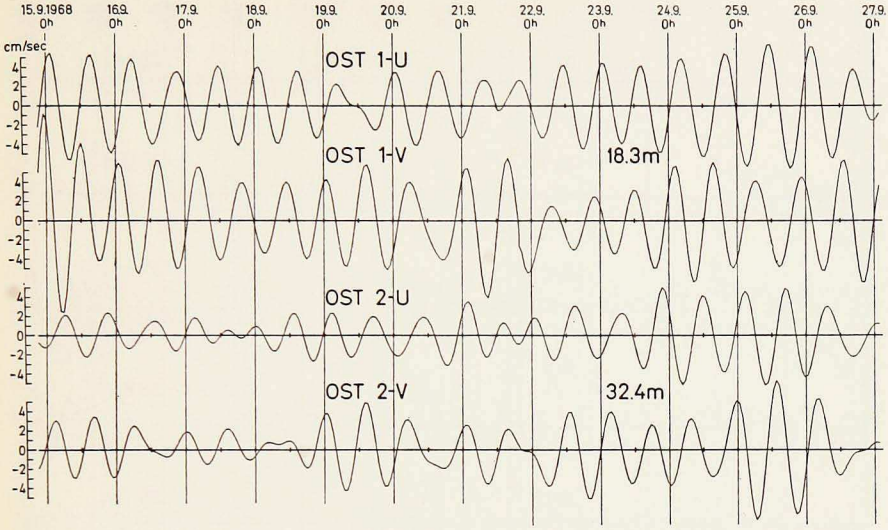

Figure 5. Eastward (u) and northward (v) inertial-period current components at St. Ost.

$k = 0.88$. The 95%-confidence bands of the phase for the pertinent k values are given in Tables II and IV.

4. *Coherence and Phase Relationships.* Fig. 5 shows that, during the first week, the inertial-period current amplitudes were greater at 18.3 m than at 32.4 m, and the maximum amplitude was at the beginning of the record; considering how the filtering procedure diminishes these amplitudes (Fig. 4), this maximum must have been even larger in the original data. During the second week of the records, at both levels, the currents at St. Ost had about the same amplitudes. Some understanding of the vertical current differences (Fig. 5) will be possible when the vertical features of the inertial-period motions are known.

Table II. Vertical coherence, k, and phase difference, ϑ, for inertial-period currents at St. Mitte, 14 September, 21 h, to 18 September, 19 h.

Sensor pairs	Current components*	k	$\vartheta°$	Sensor depth (m)
Mitte 1 – Mitte 3..	u	0.89	179	18.5 (Mitte 1)
	v	0.92	170	36.0 (Mitte 3)
Mitte 3 – Mitte 5..	u	0.88	6	
	v	0.97	350	70.0 (Mitte 5)
95%-confidence...		0.88	±5†	

* u = eastward, v = northward. † For $k = 0.9$.

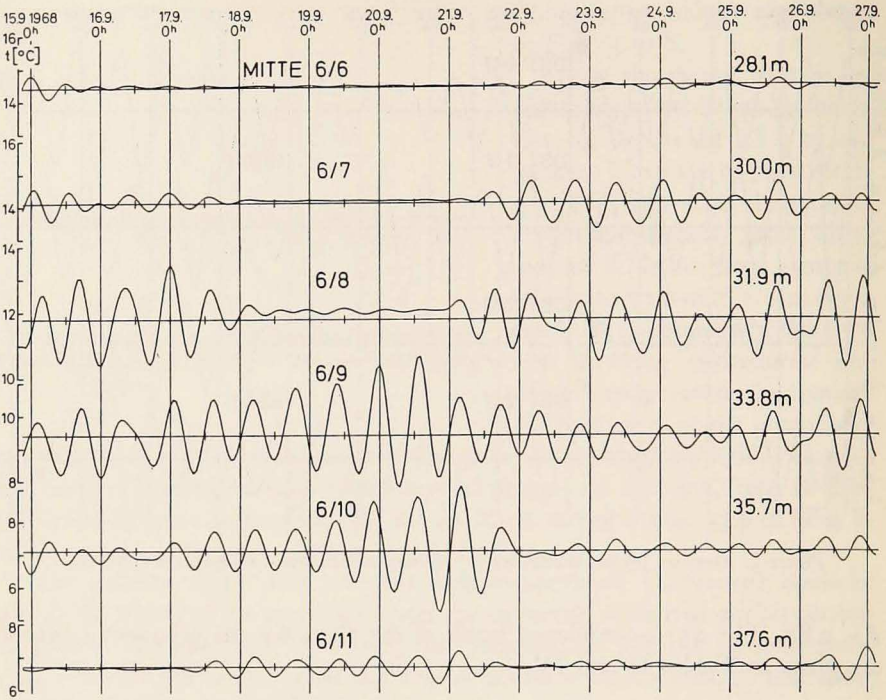

Figure 6. Inertial-period temperature fluctuations at St. Mitte.

The vertical coherences and phase relationships for the inertial currents, given in Table II, have been derived from data taken at St. Mitte with current meters No. 1 at 18.5 m, No. 3 at 36 m, and No. 5 at 70 m. For the period 14 September to 18 September, the temperature distribution did not change significantly around distribution 1, shown in Fig. 1; i.e., current meter No. 3 at St. Mitte was positioned in the lower homogeneous layer. Table I shows that the coherence values for the inertial-period currents above and below the thermocline were high compared with those for neighboring frequencies. The inertial-period currents at 36 m and 70 m, in the lower layer, were in phase, and they were in almost exact antiphase to the currents at 18.5 m. This is the current distribution for first-order internal waves in a two-layered sea.

Similar evidence for first-order internal-wave appearance has been derived from the temperature fluctuations at St. Mitte (Fig. 6); these temperature fluctuations indicate that the vertical motions are in phase throughout the thermocline. The changing vertical distribution of the temperature fluctuations shown in Fig. 6 is due to the changing temperature gradients (Fig. 1). The vertical amplitudes extend up to 1 m. The time changes in the vertical motion were not calculated because of the possible errors caused by not knowing the exact position of a sharp thermocline.

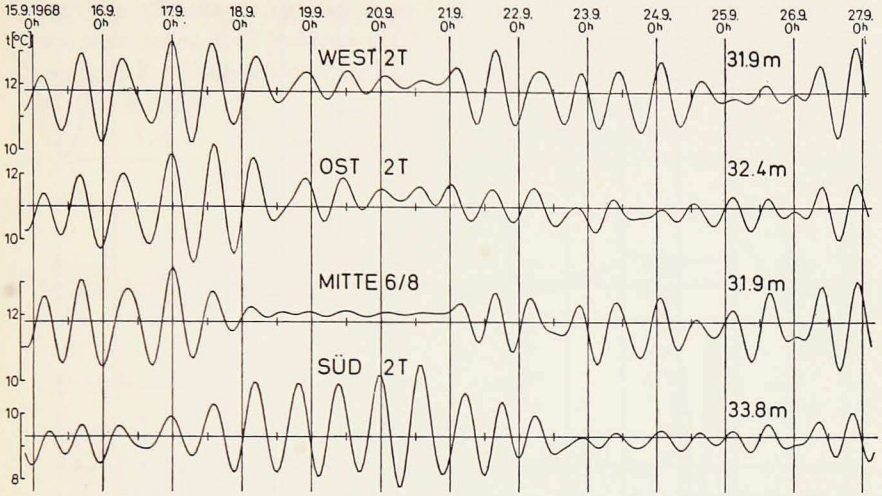

Figure 7. Inertial-period temperature fluctuations at the four stations (see Table III for spacing).

The very sharp current shear of the inertial currents can be demonstrated by comparing data from current meters No. 1 at 18.5 m and No. 2 at 32.4 m at St. Ost—i.e., within the thermocline. During the first part of the investigation (14 September to 18 September) and the last part (22 September to 27 September), the current shear occurred above meter No. 2, and the currents shown by meters No. 1 and No. 2 were almost in antiphase; however, from 18 September to 22 September, the thermocline sank below meter No. 2 (Fig. 1) and both meters showed currents nearly in phase. Correspondingly, the amplitudinal variations in the record for meter No.2 (St. Ost) in Fig. 5 were produced to a large extent by changes in the current shear.

Table III. Spatial coherence for inertial-period temperature fluctuations within the thermocline.

Sensor pairs	Recording period: 14 Sept., 21 h to 18 Sept., 19 h (coherence)	Recording period: 14 Sept., 21 h to 27 Sept., 3 h (coherence)	Distances: horiz. (km)	Distances: vert. (m)
Mitte 6/8 – Ost 2T.....	0.89	0.85	2.5	0.5
Mitte 6/8 – West 2T....	0.93	0.88	2.3	0
Ost 2T – West 2T	0.95	0.89	4.5	0.5
Süd 2T – Ost 2T.....	0.85	0.58	4.3	1.4
Süd 2T – West 2T.....	0.77	0.53	4.0	1.9
Süd 2T – Mitte 6/9.....	0.89	0.94	2.5	0
Süd 2T – Mitte 6/8.....	0.61	0.39	2.5	1.9
95%-confidence.....	0.88	0.73		

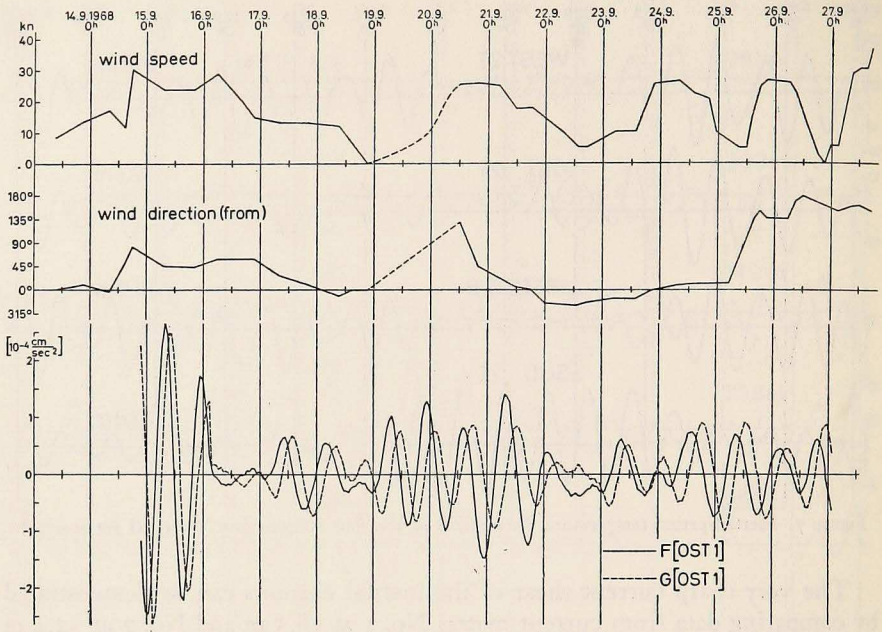

Figure 8. Wind conditions at the observation site and the time series F, G at St. Ost at 18.3 m. The dashed lines in the curves for wind speed and direction indicate that the data were derived from meteorological charts, not from ship observations.

Fig. 7 shows the inertial-period temperature fluctuations measured at 31.9 m at Sts. West and Mitte, at 32.4 m at St. Ost, and at 33.8 m at St. Süd. The spatial coherence for these fluctuations has been calculated (Table III) for two periods: for 14 September to 18 September, when the mean temperature distribution was almost constant, and for the entire record, i.e., with changing depth and shape of the thermocline. The horizontal spacings and the depth differences among the sensors are indicated in the last two columns of Table III. As shown in the second column of Table III, under uniform temperature conditions the coherence between sensors at about the same depth was very high, close to, or more than, 0.9, even at separations of 4.5 km. The depth difference of only 1.9 m between the sensors at St. Süd and St. West as well as between St. Süd and St. Mitte reduced the coherence between these stations to 0.77 and 0.61. For the values calculated from the entire record, the coherence loss with depth difference—due to the change in temperature conditions—was much greater. Whereas records from the same depth still showed coherences of about 0.9 (Table III, column 3), the coherences between the records at St. Süd and St. West fell to 0.53 and between St. Süd and St. Mitte to a value as low as 0.39.

Since these coherence values (Table III) are mainly dependent upon the sensors being located in homogeneous water during part of the time, their

Table IV. Coherence, k, and phase difference, ϑ, for inertial-period currents and time series F, G between the No. 1 meters at Sts. Mitte and Ost (sensor depth at St. Mitte 18.5 m, at St. Ost 18.3 m, horizontal distance 2.5 km); St. Mitte leads.

	Recording period			
	14 Sept., 21 h to 18 Sept., 19 h		14 Sept., 21 h to 27 Sept., 3 h	
	k	$\vartheta°$	k	$\vartheta°$
Current components { eastward...	0.99	357	0.99	358
Current components { northward .	0.93	356	0.97	357
F.....	0.58	346	0.45	17
G.....	0.64	348	0.42	11
95°-confidence.....	0.83	± 2* ±30†	0.73	± 1* ±24†

* for $k = 0.95$. † for $k = 0.50$.

value as estimates of the horizontal coherence scale of the vertical inertial-period motion (i.e., of the forced inertial waves) is low. But the high values derived from sensors located at the same depth indicate at least that the horizontal coherence scale of the forced oscillations should be large compared with the sensor spacings.

The horizontal coherence values for the inertial-period current components in the upper layer (18.5 m) and for the 2.5-km separation (upper part of Table IV) are close to one for 14 September to 18 September as well as for the entire period of study. This is shown by the relationship between the current meters No. 1 at Sts. Mitte and Ost. The phase differences between these two records are very small, as is to be expected for inertial currents.

Table V gives the spatial coherence values for records from current meters No. 2 at St. West (31.9 m), St. Ost (32.4 m), St. Süd (33.8 m), and from current meter No. 3 at St. Mitte (36.0 m). Column 2 gives the coherences for 14 September to 18 September, and Column 3 for 14 September to 27 September.[2] The horizontal and vertical separations of the current meters are given in the last two columns. The coherence values in Table V are much smaller than those derived from the current records in the upper homogeneous layer (Table IV).

Two effects were mainly responsible for this coherence loss; both effects resulted from the depth differences between the current meters, not from their horizontal separations.

First, the time variability in the depth as well as the shape of the thermocline caused depth variations in the zero value of the first-mode currents which, from their part, must have produced varying differences in amplitudes

2. The values of meter No. 3 at St. Mitte cover only the period from 14 September to 18 September because of the malfunction of this meter before the investigation ended (Table I).

Table V. Spatial coherence for inertial-period current components within the thermocline.

Sensor pairs*	Current components*	Recording period: 14 Sept., 21 h to 18 Sept., 19 h	Recording period: 14 Sept., 21 h to 27 Sept., 3 h	Distance: horiz. (km)	Distance: vert. (m)
Ost 2 – West 2	u	0.94	0.82	4.5	0.5
	v	0.89	0.86		
Süd 2 – Ost 2	u	0.88	0.87	4.3	1.4
	v	0.81	0.92		
Süd 2 – West 2	u	0.87	0.72	4.0	1.9
	v	0.73	0.71		
Mitte 3 – Ost 2	u	0.38	–	2.5	3.6
	v	0.46			
Mitte 3 – West 2	u	0.35	–	2.3	4.1
	v	0.23			
Mitte 3 – Süd 2	u	0.72	–	2.5	2.2
	v	0.83			
95%-confidence		0.88	0.73		

* u = eastward; v = westward.

and phases between current records from meters in the thermocline, even if their vertical separations were only a few meters. Consequently, the vertical coherence between these records must be reduced.

Second, the currents might have contained comparable contributions from many modes in the thermocline, where the first mode vanished, with a corresponding small vertical coherence (Hasselmann 1970). Support for the presence of this second effect can be taken from Table V, second column, lower part: the coherences between the currents recorded by meter No. 3 at St. Mitte (below the thermocline) and by meters No. 2 at Sts. West and Ost (in the thermocline), for 14 September to 18 September, are small compared with the other values in that column, although the temperature profile was rather constant during this time; i.e., the first effect was not of primary importance.

5. *Forced Oscillations.* Two theoretical investigations on the generation of near-inertial-period internal waves, starting with different assumptions, have given similar results. Crepon (1969) worked with wind-stress step functions; Hollan (1969) introduced a volume force with a bandlike horizontal distribution acting in a finite volume. In both models, internal waves with periods that are slightly below the inertial period are generated; in the course of time and with increasing distance from the discontinuity (Crepon) or excitation area (Hollan), the periods of the internal waves approach the inertial period.

Similar concepts are applicable in the present study: Internal waves generated by wind action have periods below the inertial period. Most of the energy

must be contained in the first mode, with the corresponding phase reversal of the currents at the interface (Table II). As their frequencies, ω, approach the inertial frequency, f, and as they tend to become free oscillations, the interdependence between the elevation of the thermocline, ζ, and the current speeds in the upper and lower layers, s_1 and s_2, is

$$\zeta = \frac{kh_1}{\omega} s_1 = -\frac{kh_2}{\omega} s_2,$$

with k the wave number and h_1, h_2 the depths of the upper and lower layers.

Then ζ has to decline quickly for the given s_1, s_2 with ω toward the inertial frequency, since (see section 6)

$$k \sim (\omega^2 - f^2)^{1/2}.$$

Thus the current oscillations contain more energy for the very small wave numbers than do the temperature series. This is verifiable by examining the horizontal phase differences of currents and temperature fluctuations; for the currents measured by meters No. 1 at Sts. Mitte and Ost (2.5-km separation), the mean horizontal phase difference was 2.3°. However, the temperature fluctuations measured by sensor 2 at St. Ost, compared with those measured by sensor 6/8 at St. Mitte, showed an 11° horizontal phase difference.

In order to eliminate the free oscillations,

$$F(t) = \frac{\partial u}{\partial t} - fv,$$

$$G(t) = \frac{\partial v}{\partial t} + fu$$

were determined from the time series of the eastward (u) and northward (v) current components. For the free inertial oscillations, the right-hand sides must vanish and $F(t)$, $G(t)$ should provide information about the occurrence of forced inertial oscillations.

$F(t)$ and $G(t)$, determined from the currents recorded by meter No. 1 at St. Ost (Fig. 5), are shown in Fig. 8, lower part. Amplitude spectra, like that in Fig. 2, of the F-series and G-series (not presented here) still show maximum amplitudes in the near-inertial frequency range, but the inertial-period amplitudes are no longer so predominant in $F(t)$, $G(t)$ as they were in the current records (Fig. 5). Other current fluctuations with periods in the pass-band of the two-step filter (Fig. 4) also contribute to the F-values and G-values in Fig. 8.

The wave-number spectra of $F(t)$, $G(t)$ near the inertial frequency have the maxima at finite wavelengths; this is proved by using the horizontal phase differences. The F-series and G-series determined from the current records of meters No. 1 at Sts. Mitte and Ost (2.5-km separation) in Table IV show

phase differences of more than 10°; these differences are of about the same magnitude as those derived from the temperature fluctuations shown in Fig. 7. There are, however, differences between the forced oscillations obtained in $F(t)$, $G(t)$ and the temperature fluctuations. Table IV, lower part, shows the horizontal coherence values for the F-series and G-series; they are much lower than those obtained from the temperature fluctuations, which were measured by sensors at the same depths and at similar horizontal separations (Table III). These low coherences resulted from the presence in $F(t)$, $G(t)$ of only a small number of near-inertial-period oscillations, whereas in the temperature records, near-inertial-period motions are apparent during all of the investigation (Figs. 6, 7). This means that, by computation of $F(t)$, $G(t)$, only part of the near-inertial-period current oscillations were obtained.

Let us now examine the occurrence of F and G in comparison with the change in wind conditions. The upper part of Fig. 8 shows the mean wind speed and wind direction. The use of these wind observations may be rather questionable because they were gathered with different observational methods aboard different ships at different locations near the observation site. The F-series and G-series from meter No. 1 at St. Ost (Fig. 8, lower part) show a pronounced maximum on 15–16 September. For more than 10 days before the beginning of the current measurements, the weather was very calm; therefore the sudden increase in wind speed and the simultaneous change in wind direction on 14 September must be the reason for this amplitudinal maximum.[3] It is of interest to note how quickly the forced oscillations declined relative to the currents shown in Fig. 5. After a few cycles, the energy had shifted toward the zero wave-numbers.

During the next stronger wind period, 19–20 September, again near-inertial oscillations can be observed in $F(t)$, $G(t)$. Near the end of the observational period, several wind bursts from different directions occurred so close together as to prevent clear identification of the production of forced oscillations. Furthermore, it is well known that a simple correlation between wind stress and inertial oscillations may not be expected, since a wind-stress change may enhance or destroy the inertial oscillations, this depending upon the phase relationship between the wind-stress variation and the inertial oscillations (Crepon 1969, Hasselmann 1970, Pollard and Millard 1970). The wind data used in this study are too crude to provide an insight into these phase relationships, but the simple procedure outlined above may serve as a satisfactory means of studying the occurrence of forced oscillations; it has provided evidence of their dependence on local winds.

6. *Wavelengths and Horizontal Propagation.* For a complete picture of the generation and decay processes of inertial waves, their spatial propagation and

3. It can be shown that only a small fraction of this amplitude maximum is the result of the filtering effect (illustrated in Fig. 4) on the currents shown in Fig. 5.

its dependence on the change in sea-surface conditions must be known. There are three main reasons why it is difficult to derive information about horizontal propagation of inertial-period motions from current and temperature time series.

i. In a small frequency range, from the inertial frequency up to some higher frequency, ω, the wave-numbers, k, have a continuum from zero to $k(\omega)$ for each mode. So the computed phase relationships are averages, weighted with the amplitudinal distribution in this continuum.[4]
ii. The amplitudinal distribution in the wave-number continuum changes as the frequencies of the forced oscillations approach the inertial frequency.
iii. The forced oscillations from several events may be superimposed on each other in the records.

In spite of these difficulties, the calculations of phase differences seem to have the potential of providing valuable information, if the amplitudinal distribution in the near-inertial wave-number space is similar in the records investigated. This potential is demonstrated by the vertical and horizontal phase differences for the currents and temperatures discussed in the previous sections.

In principle, determining the direction of propagation of a forced inertial thermoclinic wave should be possible from the relationship between the vertical and horizontal motion; the current component in the propagation axis should be in antiphase with the elevation of the thermocline. However, in the inertial-period currents, the zero wave-number components predominate over those that correspond to the elevation of the thermocline. Consequently, application of this method is not possible.

Therefore the propagational directions and horizontal wavelengths have been determined from the horizontal cospectra and quadrature spectra, C_i and Q_i ($i = 1 \ldots 6$), of the temperature fluctuations at the four stations. The method employed is that of the best-fitting plane wave (Munk et al. 1963). Following this method, with trial values of wave-number, k, and propagational direction, φ, a maximum of the function

$$\tilde{E}' = \sum_{i=1}^{6} C_i \cos\left[k(\xi_i \sin\varphi + \mu_i \cos\varphi)\right] + \sum_{i=1}^{6} Q_i \sin\left[k(\xi_i \sin\varphi + \mu_i \cos\varphi)\right]$$

must be determined. The pair k_0, φ_0 of $\tilde{E}'_{\max}$ is the plane wave that best fits the measured set, C_i, Q_i. (ξ_i, μ_i are the EW-coordinate and NS-coordinate differences between the station positions). The applicability of the method in the case of internal waves has been discussed by Schott (1971).

4. Normally, different modes will be mixed up in the records, as was discussed for the inertial-period current records from the thermocline; but the temperature fluctuations in the thermocline showed a clear first-mode distribution (Fig. 6).

The physical interpretation of the propagation of inertial oscillations determined in this manner requires exact information about the horizontal structure of the wind field and its time variations, but such data were not obtained in the present study. For the inertial oscillations during 14–18 September, apparently caused mainly by the wind on 14 September, a southward propagation could be determined. This direction of propagation should have been created by the front of a wind field moving southward. However, the information from the weather maps is not adequate to determine the real development of the wind field.

The horizontal wavelength was found to be 50 km. From 22 to 27 September, the same wavelength was obtained from the temperature fluctuations. So perhaps this value can be regarded as being somehow representative of the vertical inertial-period motions in the observed area. What may be the frequency deviation between the frequency, ω, of an internal wave of 50-km wavelength and the inertial frequency, f? Suppose it is a free wave; then, in the two-layered sea, this deviation is described by (Defant 1952)

$$\omega^2 - f^2 = gk^2 \frac{h_1 h_2}{h_1 + h_2} \cdot \frac{\varrho_2 - \varrho_1}{\varrho_2},$$

with k the wave-number, g the earth's gravity acceleration, h_1, h_2 the layer depths, and ϱ_1, ϱ_2 the densities of the upper and lower layers. With $(\varrho_2 - \varrho_1)/\varrho_1 = 1.3\ 10^{-3}$, $h_1 = 35$ m, $h_2 = 37$ m, $g = 9.81$ m sec^{-2}, this formula yields a 2.2% frequency increase of ω against f for the 50-km wavelength. This small deviation cannot be verified from the single records by counting the cycles or by applying the method of complex demodulation (Perkins 1970), since the Doppler effect is much greater; a 1% frequency variation near the inertial frequency only needs a mean current of 1 cm/sec along the propagational path of the internal wave, and the mean currents sometimes were of the order of 10 cm/sec and of varying directions. They were, however, very similar at the four stations so that the phase differences between the temperature records for the four stations are really caused by the propagation of the inertial waves.

7. *Summary and Conclusions.* The horizontal coherence scale of the horizontal and vertical components of inertial-period motions is large compared with the mooring separations (4.5-km maximum). The vertical profile of horizontal and vertical components has a predominent first-mode structure, but, within the thermocline, the vertical coherence of the currents is reduced by the presence of higher modes. All results are strongly dependent on changes in the density profile, which therefore has to be recorded continuously in time and with vertically closely spaced sensors. The horizontal inertial-period currents, in the mean, had almost zero horizontal wave-numbers, but it is

shown that wind-stress changes can cause frequency deviations from the inertial frequency in the current oscillations. The mean horizontal wavelength of the vertical component of the inertial-period motions was found to be about 50 km. A satisfactory interpretation of the horizontal propagation of inertial-period motions, which was not possible in this study, will be possible only if wind measurements around the current meter moorings are obtained on a large scale.

Acknowledgment. I am indebted to Klaus Hasselmann for helpful discussions on the generation and propagation of inertial oscillations.

REFERENCES

CREPON, MICHEL
1969. Hydrodynamique marine en régime impulsionnel. Pt. 3, Chap. 1. Formation d'ondes internes de longues periodes dans un océan à deux couches. Cah. Oceanogr., *221*(9): 863–877.

DEFANT, ALBERT
1952. Über interne Wellen, besonders solche mit Gezeitencharakter. Dtsch. hydrogr. Z., 5(5): 231–245.

DEUTSCHER WETTERDIENST
1968a. Täglicher Wetterbericht, Teil A. Karten. Offenbach. *93*: 258–271.
1968b. Täglicher Wetterbericht, Schiffsbeobachtungen. Hamburg. *93*: 258–271.

DOODSON, A. T., and H. D. WARBURG (Editors)
1941. Admirality manual of tides. London.

GRANGER, C. W. J., and M. HATANAKA
1964. Spectral analysis of economic time series. Princeton University Press, Princeton, N. J. 299 pp.

HASSELMANN, KLAUS
1970. Wavedriven inertial currents. Geophys. fluid Dyn., *1*(4): 463–502.

HOLLAN, ECKARD
1969. Die Veränderlichkeit der Strömungsverteilung im Gotland-Becken am Beispiel von Strömungsmessungen im Gotland-Tief. Kieler Meeresforsch., *25*(1): 19–70.

MUNK, W. H., G. R. MILLER, F. E. SNODGRASS, and N. F. BARBER
1963. Directional recording of swell from distant storms. Philos. Trans., (A) *255*: 508–584.

PERKINS, H. T.
1970. Inertial oscillations in the Mediterranean. Ph. D. Thesis, M.I.T. and WHOI; 155 pp.

POLLARD, R. T., and R. C. MILLARD
1970. Comparison between observed and simulated wind-generated inertial oscillations. Deep-sea Res., *17*(4): 813–821.

SCHOTT, FRIEDRICH
1971. On horizontal coherence and internal wave propagation in the North Sea. Deep-sea Res., 18.

SCOR Working Group on Continuous Current Velocity Measurements
1969. An intercomparison of some current meters. UNESCO Techn. Pap. Mar. Sci., *11*; 70 pp.

Tomczak, Matthias Jr.
1969. Über interne Trägheitsbewegungen in der westlichen Ostsee. Dtsch. hydrogr. Z., *22*: 158–162.

Webster, Ferris
1968. Observations of inertial-period motions in the deep sea. Rev. Geophys., *6*(*4*): 473–490.